

# The Large-Scale Modulation of Subtropical Cyclogenesis in the Central and Eastern Pacific Ocean

JASON A. OTKIN AND JONATHAN E. MARTIN

*Department of Atmospheric and Oceanic Sciences, University of Wisconsin—Madison, Madison, Wisconsin*

(Manuscript received 25 April 2003, in final form 4 February 2004)

## ABSTRACT

An analysis of the composite large-scale circulation associated with periods of enhanced (active) or diminished (inactive) cyclogenesis in the subtropical central and eastern Pacific Ocean is presented. Composites were constructed using surface and tropospheric analyses from the ECMWF Tropical Ocean Global Atmosphere (TOGA) dataset for 10 Northern Hemisphere cool seasons (1986–96). Active periods of subtropical cyclogenesis were defined to be periods in which two or more cyclones developed in close succession to each other, while inactive periods were defined to be periods of at least 10-days duration during which no cyclones with a subtropical origin were present in the Pacific basin.

The analysis revealed that the occurrence of subtropical cyclones in the central and eastern Pacific Ocean is strongly linked to the strength and location of the Asian jet, with active periods characterized by a weaker, zonally retracted Asian jet while inactive periods are characterized by a stronger, zonally elongated Asian jet. Consideration of the stationary wavenumber,  $K_s$ , showed that the strong, zonally elongated jet characterizing inactive periods produced a continuous waveguide across the Pacific basin that severely limited the equatorward propagation of upper-level cyclones into the subtropical Pacific. However, the zonally retracted jet during active periods was associated with a poorly organized, or “leakier,” waveguide across the Pacific, which produced a decidedly more favorable situation for the equatorward propagation of upper-level cyclones leaving the exit region of the Asian jet.

Outgoing longwave radiation data were used to explore the potential link between anomalous convection in the tropical Pacific and the occurrence of active and inactive periods. A detailed analysis of each active and inactive period revealed that only 55% of the periods were characterized by the theoretically expected distribution of anomalous convection across the tropical Pacific (deemed “correct”) and that 30% of the periods were actually characterized by the exact opposite distribution (deemed “incorrect”). During correct active and correct inactive periods, Rossby wave dispersion away from anomalous tropical convection in the central Pacific is associated with an extratropical response resembling the Pacific–North American pattern. Further analysis revealed that the lack of subtropical cyclones during most incorrect inactive periods was associated with a strengthened and zonally elongated Asian jet. The observed broadening and weakening of the Asian jet that occurs during the transition to incorrect active periods suggests that barotropic energy conversions may play an important role in fostering a large-scale environment conducive to the frequent development of subtropical cyclones during incorrect active periods.

## 1. Introduction

During the Northern Hemisphere cool season, cyclones frequently develop in the subtropical central and eastern Pacific (SCEP) Ocean. Simpson (1952) provided the first analysis of the structure and evolution of these subtropical cyclones, known as kona storms<sup>1</sup> in Hawaii. By using standard surface observations and a limited number of upper-air soundings, he revealed that kona

storms possess a cold-core structure and are primarily associated with the intrusion of upper-level disturbances of extratropical origin into the subtropical easterlies. All subsequent examinations of kona storms have focused on case studies of individual cyclones (e.g., Ramage 1962; Businger et al. 1998; Wang et al. 1998; Morrison and Businger 2001; Martin and Otkin 2004) or examined the influence that kona storms have on the climate of the Hawaiian Islands (e.g., Lyons 1982; Chu et al. 1993; Kodama and Barnes 1997).

More recently, Otkin and Martin (2004, hereafter denoted OM) have examined 10 continuous years of sea level pressure (SLP) data in the process of compiling an updated climatology of kona storms. Their analysis of the kona life cycle revealed that the initial development of most kona storms (96%) occurs along a cold front that extends southward from a midlatitude cyclone

<sup>1</sup> The terms “kona storm” and “subtropical cyclone” are used interchangeably in this paper.

*Corresponding author address:* Dr. Jonathan E. Martin, Department of Atmospheric and Oceanic Sciences, University of Wisconsin—Madison, 1225 W. Dayton Street, Madison, WI 53706.  
E-mail: jon@aos.wisc.edu

and is preceded by the intrusion of a positive upper-tropospheric potential vorticity anomaly of extratropical origin into the subtropics. As the surface cyclone intensifies, an anticyclone to the northwest rapidly propagates to the east and isolates the surface cyclone from cold air sources to the north. This aspect of the kona life cycle distinguishes these cyclones from the typical extratropical cyclone and also signals that a mature kona storm has developed. The mature kona storm is characterized by a cutoff disturbance in the upper troposphere and a substantial region of warm surface potential temperature anomalies to the east of the surface cyclone. The final stage of the kona life cycle is typically characterized by the merger of the kona storm with a transient midlatitude trough or, less often, by the slow decay of the mature cyclone.

In his more limited climatology of kona storms, Simpson (1952) revealed that approximately four kona storms developed during an average winter season. However, by using a more recent dataset that contains better spatial coverage across the Pacific Ocean and considering a slightly larger domain, OM have shown that an average of 10 subtropical cyclones occur during each boreal cool season. Inspection of the cyclone frequency during individual months and years revealed substantial month-to-month and interannual variability. In order to discern the underlying physical processes that produce the observed temporal variations in kona activity, the present paper contrasts the large-scale circulation features present across the Pacific basin during periods that are characterized by the frequent or infrequent occurrence of subtropical cyclones.

The study is organized as follows. In section 2, we review the characteristics of relevant teleconnection patterns and provide an overview of the empirical and theoretical evidence for tropical–extratropical interaction in the Pacific basin. The definitions of active and inactive periods of subtropical cyclogenesis and a description of the data used for the study are provided in section 3. In section 4, we examine the composite large-scale circulations associated with active and inactive periods and also illustrate the important role of the Asian jet in modulating the frequency of subtropical cyclones. Section 5 examines an additional stratification of the active and inactive periods made with respect to the phase of outgoing longwave radiation (OLR) anomalies in the equatorial Pacific. Possible mechanisms underlying the broadening and weakening of the Asian jet observed during the transition to active periods are also considered. Discussion of results, suggestions for future work, and conclusions follow in section 6.

## 2. Historical background

Empirical evidence for the existence of recurrent low-frequency circulation patterns in the troposphere has been provided by numerous teleconnection studies. The seminal study of Wallace and Gutzler (1981) utilized

correlation matrices derived from 15 yr of Northern Hemisphere 500-hPa geopotential height data to present evidence of the existence of five fundamental low-frequency height anomaly patterns. Among these five patterns, only the Pacific–North American (PNA) pattern will be considered in the present study. Subsequent studies by Blackmon et al. (1984a,b) revealed that low-frequency teleconnection patterns can be classified into intermediate (with periods between 10 and 30 days) and long (with periods exceeding 30 days) time scales. The intermediate scales are characterized by wave trains that originate in the climatological mean entrance regions of both the Asian and North American jets. These wave trains show a preference for eastward dispersion through geographically fixed waveguides associated with the mean jets and subsequent southeastward curvature toward the subtropics in the exit regions of each jet. The long time-scale fluctuations are dominated by dipolar patterns that straddle the climatological mean jet exit regions and exhibit well-defined, geographically fixed teleconnection patterns.

Numerous observational studies have shown that interannual tropical sea surface temperature anomalies associated with ENSO are closely linked to changes in the extratropical circulation (e.g., Horel and Wallace 1981; Geisler et al. 1985; Lau and Phillips 1986; Kidson et al. 2002). On intraseasonal time scales, several studies have explored the connection between the Madden–Julian Oscillation (MJO) and the extratropical circulation. Using 10 yr of OLR and 250-hPa streamfunction data, Weickmann et al. (1985) showed that as enhanced convection associated with the MJO propagated eastward into the western tropical Pacific, an anomalous subtropical cyclone shifted eastward into the central Pacific while an anticyclonic anomaly developed over the extratropical North Pacific. However, with enhanced convection over the central equatorial Pacific, the opposite pattern occurred as an anomalous subtropical anticyclone–extratropical cyclone dipole developed in the central Pacific. The reversal of this circulation anomaly dipole in the central Pacific has been shown to exert a statistically significant influence on the strength and location of the Asian jet (Knutson and Weickmann 1987). Kiladis and Weickmann (1997) have also found that tropical convection in the western Pacific appears to force an enhanced Hadley circulation into the Asian jet that leads to a downstream acceleration of the jet. Therefore, by modulating the strength and location of the Asian jet, tropical convection associated with the MJO can indirectly influence the midlatitude circulation.

Additional evidence for tropical–extratropical interaction on intraseasonal time scales and for a connection between anomalous tropical convection and the realization of the PNA pattern in the extratropical circulation has been provided by a number of prior studies (e.g., Kousky 1985; Livezey and Mo 1987; Hoerling et al. 1997; Higgins and Mo 1997; Wang and Fu 2000). This empirical evidence is complemented by theoretical un-

derstanding of the forcing of the extratropical circulation by tropical convection. Hoskins and Karoly (1981) found that heating associated with deep convection in the low latitudes leads to the development of a Rossby wave train emanating away from the region of heating. Within this wave train, the longer waves have a strong poleward and eastward propagation and can effect regions far removed from the region of deep convection. They showed that the height perturbations associated with these wave trains have an equivalent barotropic structure away from the Tropics and acquire a spatial pattern very similar to the PNA pattern. Thus, their theoretical results affirm the empirical suggestion that direct forcing of the PNA pattern by tropical convection is possible.

Several subsequent observational studies, however, have struggled to uncover a direct link between tropical convection and the extratropical circulation (e.g., Dole and Black 1990; Schubert and Park 1991; Hsu and Lin 1992), suggesting that mechanisms other than Rossby wave dispersion away from a tropical heat source may be important in forcing the PNA pattern and in exciting large responses in the exit region of the Asian jet. Specifically, Schubert and Park (1991) speculated that the PNA pattern was maintained by the mean flow through barotropic energy exchanges.

Simmons et al. (1983) have presented evidence suggesting that barotropic instability in the exit region of the Asian jet can trigger a response resembling the PNA pattern. By using a barotropic model linearized about the January 300-hPa climatological mean flow, they found that structures resembling the PNA pattern tend to recur in response to localized forcings throughout the Tropics and subtropics. The relative insensitivity of the extratropical response to the longitudinal position of the forcing suggests that the Tropics may only have an indirect effect on the PNA pattern and the extratropical circulation, an inference consistent with the observational study of Schubert and Park (1991). Recent work by Cash and Lee (2001) and Feldstein (2002) has focused on linear nonmodal growth as another possible mechanism for the growth of PNA-like patterns.

Considering the wealth of evidence provided by these studies, it is apparent that a variety of physical mechanisms might reasonably produce or maintain an extratropical response similar to the PNA pattern. The fact that the southwest center of the PNA pattern lies across a large portion of the SCEP suggests that some of these mechanisms could strongly modulate the occurrence of subtropical cyclones by controlling the phase of the PNA pattern. Therefore, the present paper compares and contrasts the large-scale circulations associated with periods that are characterized by the frequent or infrequent occurrence of subtropical cyclones in the SCEP.

### 3. Data and methodology

In the present study, the European Centre for Medium-Range Weather Forecasts (ECMWF) Tropical

Ocean Global Atmosphere (TOGA) dataset and the interpolated OLR dataset compiled by the National Oceanic and Atmospheric Administration (NOAA) were employed. The ECMWF TOGA dataset consists of twice-daily sea level and standard pressure level analyses on a global domain with 2.5° latitude–longitude resolution. Ensuing analyses utilize data at sea level, 700, and 300 hPa only. The NOAA OLR dataset consists of daily OLR analyses with global 2.5° latitude–longitude resolution obtained from the average of twice-daily OLR measurements taken from the NOAA polar-orbiting satellites. For a detailed description of the quality control method and interpolation scheme used to produce the NOAA OLR dataset the reader is referred to Liebmann and Smith (1996).

Following OM, sea level pressure analyses for 10 boreal cool seasons (October–March) from 1986 to 1996 were used to subjectively identify subtropical cyclones in the central and eastern Pacific Ocean.<sup>2</sup> A cyclone was defined to be a minimum in the sea level pressure field surrounded by at least one closed isobar (analyzed at 2-hPa intervals). To qualify as a subtropical cyclone, the surface cyclone also had to initially develop within a portion of the SCEP (shown in Fig. 1) and then maintain a closed sea level isobar for a minimum of 48 h. All surface cyclones that initially developed outside of the subtropical Pacific before propagating into the SCEP were not considered to be subtropical cyclones. In addition, tropical cyclones were removed by comparing cyclone locations to the Hurricane Best Track Files for the eastern Pacific obtained from the National Weather Service's Tropical Prediction Center. The initial positions of the 101 cyclones that satisfied these requirements are shown in Fig. 1.

In section 1, it was stated that substantial month-to-month and interannual variability of subtropical cyclone activity occurs in the central and eastern Pacific. To better illustrate this variability, a daily time series of subtropical cyclone occurrence for each of the 10 cool seasons is presented in Fig. 2. It is evident that certain periods are characterized by a substantial number of cyclones (*active periods*) while other periods are totally void of cyclones (*inactive periods*). In order to provide an objective measure of this cyclone variability, active periods were defined to be periods in which two or more cyclones sequentially developed with a maximum of 10 days separation between the final time of one cyclone and the initial time of another. Inactive periods were defined to be periods of at least 10 days duration, with a 5-day boundary at both the front and back ends of the period, in which no cyclones with a subtropical origin were present within the Pacific basin. With these definitions, 28 active and 25 inactive periods (indicated by shading in Fig. 2) were identified (Table 1). Although the length of these periods varied greatly, they were

<sup>2</sup> Although Otkin and Martin (2004) examined 10 continuous years of data, this study only employs data from the 10 cool seasons.

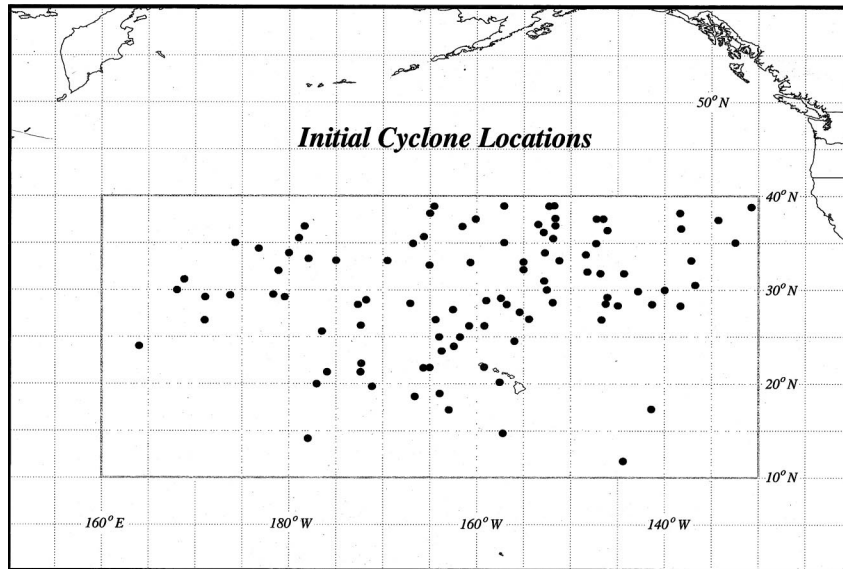


FIG. 1. Black dots represent the initial locations of the subtropical cyclones considered in the analysis. Rectangular box is the SCEP domain referred to in the text.

generally persistent features with an average length of 2 weeks for active periods and 1 month for inactive periods. Together, these 53 periods made up 68%<sup>3</sup> of the total number of days during the 10 cool seasons. Furthermore, the 28 active periods contained 83 of the 101 cool season subtropical cyclones identified by OM.

<sup>3</sup> Inclusion of the 250 days associated with the 5-day boundaries at the front and back ends of the inactive periods increases the total number of days to 82%.

#### 4. Composite active and inactive periods

##### a. Composite tropospheric conditions

As a first step in characterizing the basin-scale flow structures associated with subtropical cyclone development, a comparison of the composite large-scale features associated with active and inactive periods was made. The composites described in this section were constructed by averaging all of the data in the entire samples of active and inactive periods, respectively. In

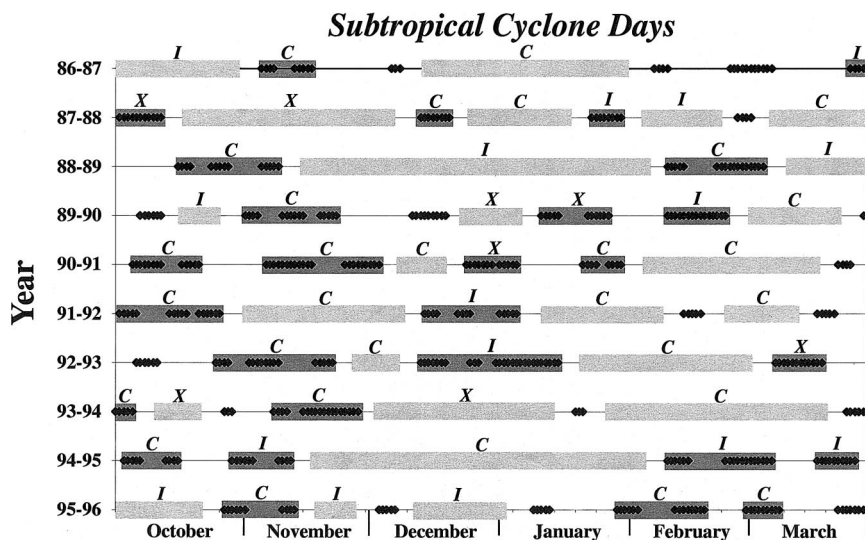


FIG. 2. Time series of subtropical cyclone activity during cool seasons (Oct–Mar) from 1986 to 1996. Black diamonds represent days on which cyclones with a subtropical origin were found in the Pacific basin. Light (dark) shading identifies the inactive (active) periods defined in the text. The letters “C,” “I,” and “X” correspond to the “correct,” “incorrect,” and indeterminate periods described in the text.

TABLE 1. The number and average length (days) of the active and inactive periods of subtropical cyclogenesis identified during the 10-yr climatology. See text for the definitions of active and inactive periods.

Period	No. of events	Avg length
Active	28	16.4
Inactive	25	31.3

the upper troposphere (Fig. 3), inactive periods are characterized by a broad trough across the western Pacific and a narrow, high-amplitude ridge over western North America (Fig. 3a). Active periods, however, are associated with a westward shift of the height pattern and are characterized by a narrow trough over eastern Asia and a broad ridge across the eastern Pacific (Fig. 3b). The westward shift of the height field from inactive to active periods is accompanied by a dramatic change in the strength and location of the Asian jet, with inactive periods characterized by an intense, zonally elongated jet extending across most of the Pacific basin (Fig. 3c) while a weaker, zonally retracted jet characterizes active periods (Fig. 3d).

In the lower troposphere, inactive periods are characterized by a narrow ridge over western North America and a broad trough across most of the North Pacific

(Fig. 4a). This height pattern stands in sharp contrast to the broad ridge over the eastern Pacific and the much smaller zonal extent and westward displacement of the Pacific trough during active periods (Fig. 4b). In the SLP field, inactive periods are characterized by a deep Aleutian low (Fig. 4c) while active periods are associated with a weakened and westward-shifted Aleutian low and by an enhanced subtropical trough near Hawaii (Fig. 4d).

Comparison of Figs. 3 and 4 indicates that the composite large-scale patterns are very different for active and inactive periods. To better illustrate these differences, Fig. 5 presents difference fields constructed by subtracting the composite inactive fields from the composite active fields. The resulting differences demonstrate that active periods are characterized by a weakened Aleutian low and subtropical high (Fig. 5a) at sea level. At 700 hPa, the difference fields reveal a subtropical trough over the central Pacific and a ridge over the North Pacific (Fig. 5b). In the upper troposphere, active periods are characterized by a weakened Asian jet (Fig. 5c) and are associated with the development of a stronger subtropical trough and extratropical ridge (Fig. 5d) than in the lower troposphere. Thickness differences in the 300–700-hPa layer (not shown) indicate that these height centers possess a cold-core equivalent barotropic structure with a correspondence between pos-

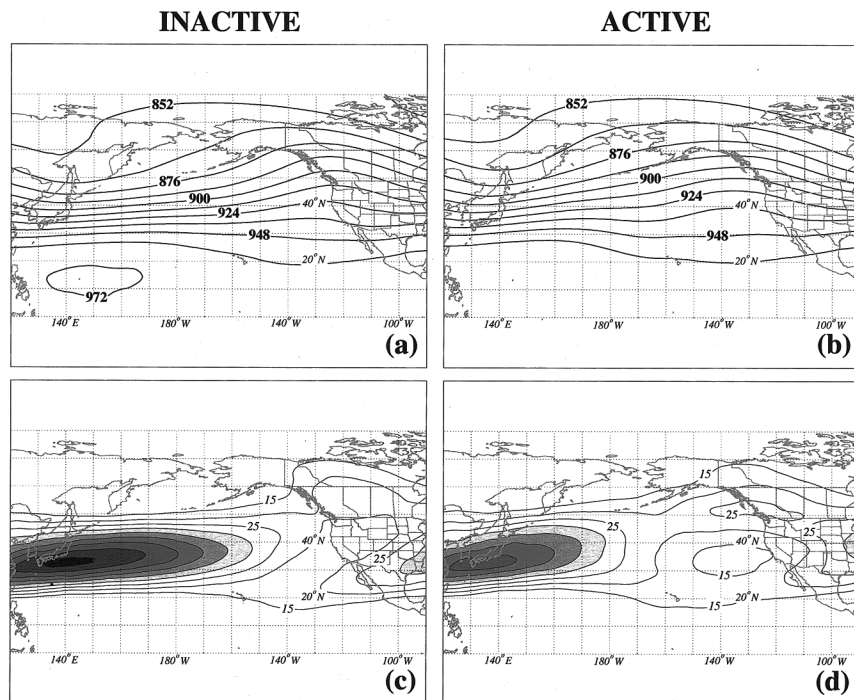


FIG. 3. (a) Composite 300-hPa geopotential height for inactive subtropical cyclogenesis periods. Solid lines are geopotential height labeled in dam and contoured every 12 dam. (b) As in (a), but for active subtropical cyclogenesis periods. (c) Composite 300-hPa isotachs for inactive subtropical cyclogenesis periods. Solid lines are isotachs labeled in  $m s^{-1}$ , contoured every  $5 m s^{-1}$  beginning at  $15 m s^{-1}$  and shaded for values above  $30 m s^{-1}$ . (d) As in (c), but for active subtropical cyclogenesis periods.

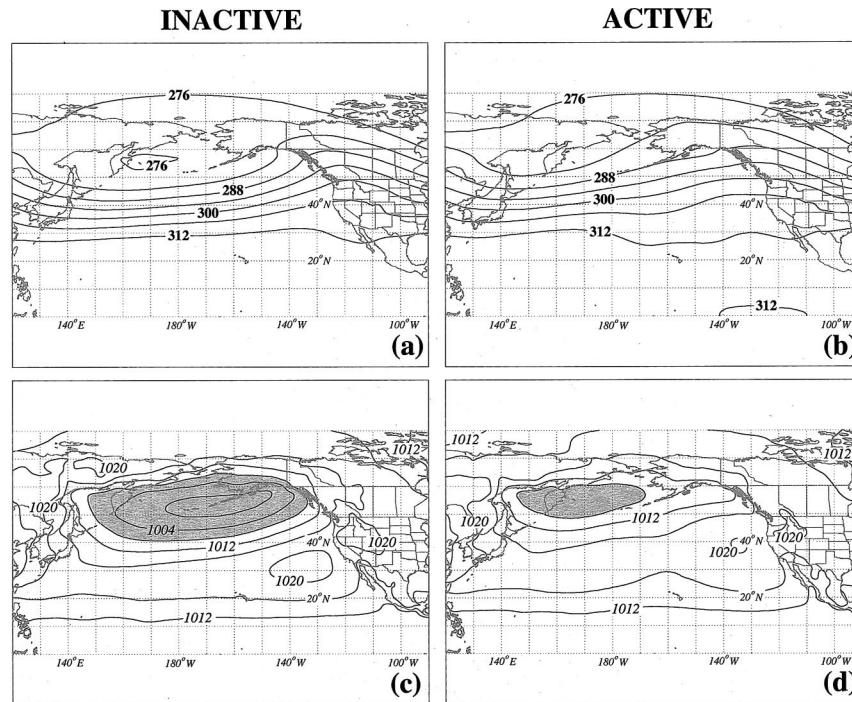


FIG. 4. (a) Composite 700-hPa geopotential height for inactive subtropical cyclogenesis periods. Solid lines are geopotential heights labeled in dam and contoured every 6 dam. (b) As in (a), but for active subtropical cyclogenesis periods. (c) Composite SLP for inactive subtropical cyclogenesis periods. Solid lines are sea level isobars labeled in hPa, contoured every 4 hPa and shaded for values less than or equal to 1008 hPa. (d) As in (c), but for active subtropical cyclogenesis periods.

itive height differences and positive thickness differences (i.e., warm ridges and cold troughs). It is also evident that the pattern of height difference centers across the central Pacific and North America (Figs. 5b,d) strongly resembles the PNA pattern. This height difference pattern indicates that active periods are associated with the negative phase of the PNA pattern whereas inactive periods are associated with the positive phase. Furthermore, the presence of a well-developed PNA pattern supports the suggestion by Chu et al. (1993) that changes in the large-scale circulation associated with opposite phases of the PNA pattern may provide an effective control on the presence or absence of subtropical cyclones in the SCEP.

#### b. Asian jet waveguide

A number of prior studies (e.g., Branstator 1983; Kiladis 1998; Matthews and Kiladis 1999) have shown that the position and intensity of the Asian jet strongly modifies the Pacific storm track by acting as an effective waveguide for cyclone activity. A diagnostic parameter that is particularly useful in illustrating the effect of this waveguide is the stationary Rossby wavenumber,  $K_s$ , given by

$$K_s = \sqrt{\frac{\beta_*}{\bar{U}}}, \quad (1)$$

where  $\beta_*$  represents the meridional gradient of absolute vorticity associated with the basic-state zonal wind,  $\bar{U}$  [i.e.,  $\beta_* = \beta - (\partial^2 \bar{U} / \partial y^2)$ ], and  $K_s$  represents the total wavenumber at which a barotropic Rossby wave is stationary at a given location with respect to the background zonal flow. Hoskins and Ambrizzi (1993) have shown that Rossby waves are always refracted toward regions of larger  $K_s$  values. Thus, since  $K_s$  is maximized along the major zonal jets where  $\beta_*$  is large relative to  $\bar{U}$ , the jets act as an effective waveguide for cyclone activity. Although this theory only applies to stationary Rossby waves, Yang and Hoskins (1996) have shown that a modified  $K$  can still provide useful information to describe the effect of the background flow on the propagation of transient Rossby waves. Therefore, from a distribution of  $K_s$ , the location of *waveguides* for stationary Rossby waves can be inferred and then used to qualitatively determine the effect of structural changes in the Asian jet in modulating the occurrence of cyclones in the SCEP.

By using (1) and the mean 300-hPa zonal wind fields characterizing the composite active (Fig. 3d) and inactive (Fig. 3c) periods, basinwide distributions of  $K_s$

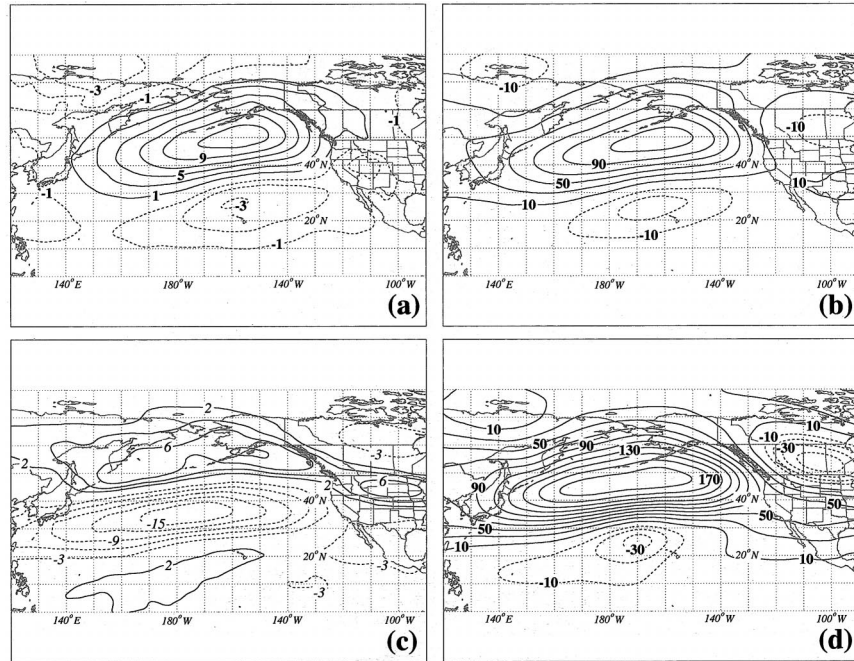


FIG. 5. (a) Mean SLP difference; composite active minus composite inactive periods. Solid (dashed) lines are positive (negative) differences labeled in hPa and contoured every 2 (1) hPa beginning at 1 (−1) hPa. (b) The 700-hPa geopotential height difference; composite active minus composite inactive periods. Solid (dashed) lines are positive (negative) differences labeled in m and contoured every 20 (10) m beginning at 10 (−10) m. (c) The 300-hPa zonal wind speed difference; composite active minus composite inactive periods. Solid (dashed) lines are positive (negative) differences labeled in  $m s^{-1}$  and contoured every 2 (3)  $m s^{-1}$  beginning at 2 (−3)  $m s^{-1}$ . (d) The 300-hPa geopotential height difference; composite active minus composite inactive periods. Solid (dashed) lines are positive (negative) differences labeled in m and contoured every 20 (10) m beginning at 10 (−10) m.

were calculated (Fig. 6). During inactive periods (Fig. 6a), a continuous band of high  $K_s$  associated with the zonally elongated Asian jet extends across the entire Pacific between 30° and 40°N. This demonstrates that for cyclones originating along the Asian jet, the jet acts as an effective waveguide that strongly limits the equa-

toward propagation of cyclones into the SCEP. However, during active periods (Fig. 6b), the waveguide appears to be less well organized, or “leakier,” with evidence of a split flow pattern across the eastern Pacific. This situation is decidedly more favorable for the equatorward propagation of upper-level waves (i.e., surface-

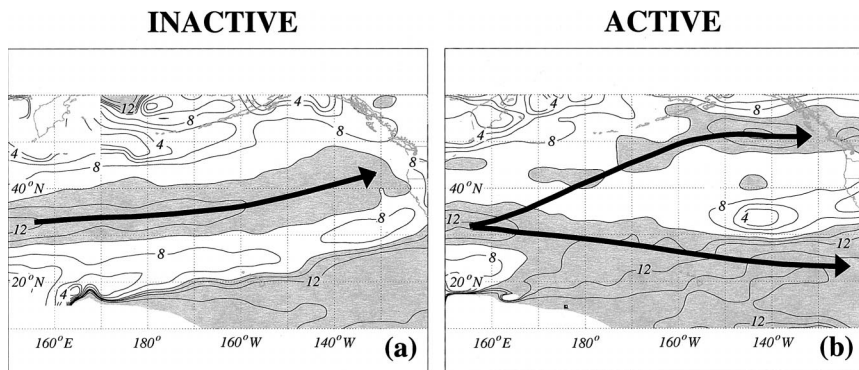


FIG. 6. Stationary wavenumber,  $K_s$ , calculated from the 300-hPa zonal wind for (a) composite inactive periods and (b) composite active periods;  $K_s$  is contoured at intervals of 2 from 0 to 20 along with the value at 11. Gray shading indicates regions where  $K_s$  is greater than 10 but less than 20. The black arrows roughly indicate axes of maximum  $K_s$ , which act as waveguides for disturbances traversing the Pacific.

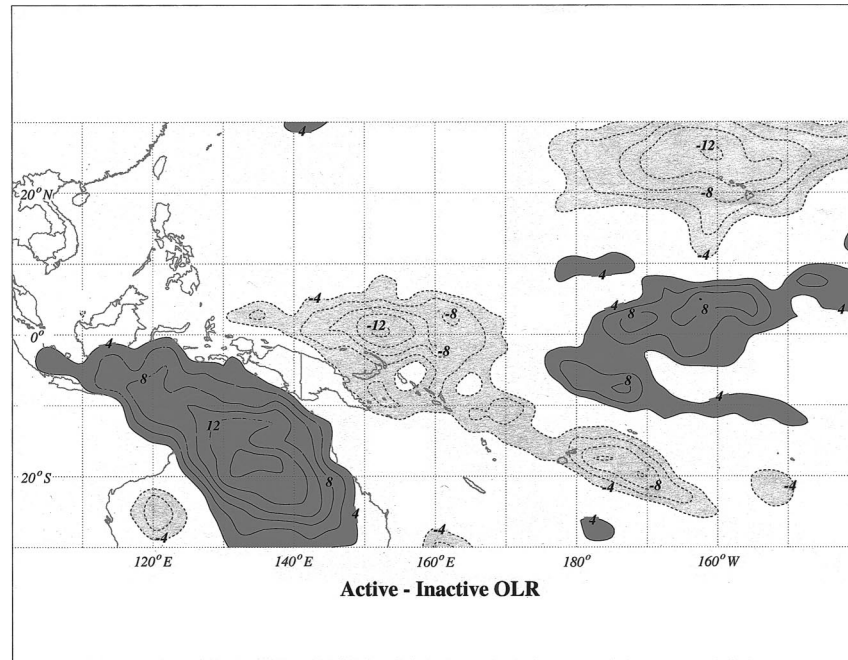


FIG. 7. Composite OLR differences between active and inactive subtropical cyclogenesis periods. Dark (light) shading with solid (dashed) lines represents positive (negative) differences in OLR labeled in  $\text{W m}^{-2}$  and contoured every  $2 \text{ W m}^{-2}$  beginning at  $4$  ( $-4$ )  $\text{W m}^{-2}$ .

cyclone spawning disturbances) into the SCEP. Thus, the clear contrast of  $K_s$  between the composite active and inactive periods illustrates the importance of the strength and location of the Asian jet in modulating the occurrence of subtropical cyclones in the SCEP.

### c. OLR

As discussed in section 2, a large body of prior work has examined the connection between tropical convection and the extratropical circulation. Those results support the suggestion that changes in the distribution of tropical convection associated with different phases of ENSO or the MJO could modulate the occurrence of subtropical cyclones by producing an environment that was either more or less favorable for cyclone development in the SCEP. For instance, it is reasonable to infer that suppressed (enhanced) tropical convection in the central Pacific would be associated with active (inactive) periods because of the generation of an anomalous subtropical trough (ridge) by Rossby wave dispersion away from the tropical convection. OLR data have been widely used to represent the intensity and distribution of tropical convection with positive (negative) OLR anomalies occurring during periods of suppressed (enhanced) tropical convection. Thus, in order to explore the possible relationship between anomalous tropical convection and the occurrence of active and inactive periods, composite OLR anomaly fields were constructed for the active and inactive periods. Daily OLR anomalies used to construct these composite OLR

anomaly fields were calculated by subtracting the climatological monthly mean from the daily OLR data.

Since it was found that the composite OLR anomaly distributions for active and inactive periods are nearly dipoles of each other, we present only the composite difference OLR field in the equatorial Pacific (Fig. 7). The zonally oriented OLR dipole represented by positive OLR differences in the central Pacific and negative OLR differences in the western Pacific suggests that active (inactive) periods are associated with suppressed (enhanced) convection in the central Pacific and enhanced (suppressed) convection in the western Pacific and along the South Pacific convergence zone. The composite OLR anomalies characterizing the active and inactive periods represent the distributions of anomalous convection that might be expected if Rossby wave dispersion away from tropical convection were the dominant modulator of subtropical cyclone activity. However, a closer inspection of the individual active and inactive periods revealed that nearly 45% of the periods did not fit this composite OLR distribution and that nearly a third of the periods were actually characterized by OLR anomalies exactly opposite to that expected from Rossby wave dispersion theory (Table 2). This suggests that, although the location and intensity of tropical convection plays an important role in forcing the extratropical circulation during many of the active and inactive periods, alternative processes must account for the presence or absence of subtropical cyclones during other periods. We examine this issue in section 5.

TABLE 2. The number of correct, incorrect, and indeterminate periods identified during the 10-yr climatology. The average lengths (days) of the correct and incorrect periods are also given. See text for the definitions of correct, incorrect, and indeterminate periods.

Period	Correct		Incorrect		Indeterminate
	No. of events	Avg length	No. of events	Avg length	No. of events
Active	16	17.4	8	16.1	4
Inactive	13	34.7	8	26.8	4

**5. Composite correct and incorrect periods**

Given the lack of uniformity among the individual active and inactive periods with respect to the distribution of anomalous tropical convection, an additional composite grouping was adopted. We define “correct” active (inactive) periods to be those with suppressed (enhanced) tropical convection in the central Pacific and enhanced (suppressed) convection in the western Pacific. Conversely, “incorrect” active (inactive) periods are characterized by enhanced (suppressed) convection in the central Pacific and suppressed (enhanced) convection in the western Pacific. With these definitions, 16 (13) correct active (inactive) and 8 (8) incorrect active (inactive) periods (identified with labels “C” or “I” in Fig. 2) were identified from the original sample of active and inactive periods (Table 2). In addition,

since four active and four inactive periods did not possess a well-defined OLR anomaly dipole (identified with the label “X” in Fig. 2), they will not be included in any subsequent composites.

Inspection of Fig. 2 indicates that the occurrence of correct and incorrect periods exhibits a strong seasonal bias, with the majority of incorrect active periods occurring during the winter while incorrect inactive periods are more common in the fall. Therefore, in order to remove the seasonal cycle from the analysis of correct and incorrect periods, anomalous OLR and anomalous 300-hPa height and zonal wind fields were calculated by subtracting the climatological monthly mean from the daily or twice-daily data, respectively. The resultant anomalies were then averaged for each sample to produce the composites presented in this section.

*a. OLR fields*

OLR anomalies for correct and incorrect periods are shown in Fig. 8. Based upon our definition of correct and incorrect periods, it is not surprising that the spatial distribution of OLR anomalies associated with correct (incorrect) active periods is nearly identical to that associated with incorrect (correct) inactive periods. These anomalous OLR distributions clearly indicate that the small magnitude of the composite OLR difference field (Fig. 7) can be attributed to the superposition of op-

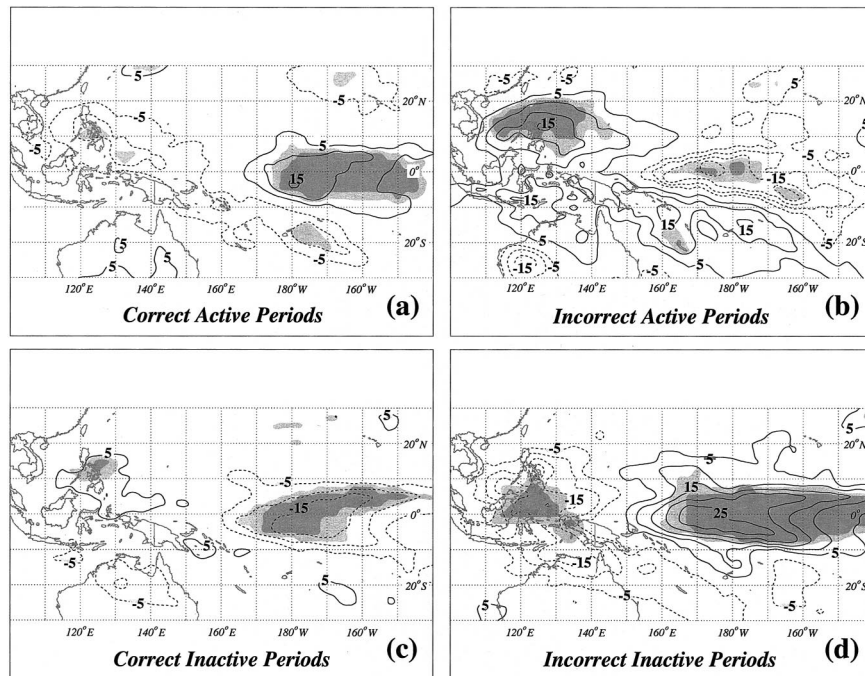


FIG. 8. (a) OLR anomalies for correct active periods. Positive (negative) anomalies are labeled in  $W m^{-2}$ , indicated by solid (dashed) lines contoured every  $5 W m^{-2}$  beginning at  $5 (-5) W m^{-2}$ . The light (dark) shading indicates regions where the features are statistically significant at the 95% (99%) level. (b) As in (a), but for incorrect active periods. (c) As in (a), but for correct inactive periods. (d) As in (a) but for incorrect inactive periods.

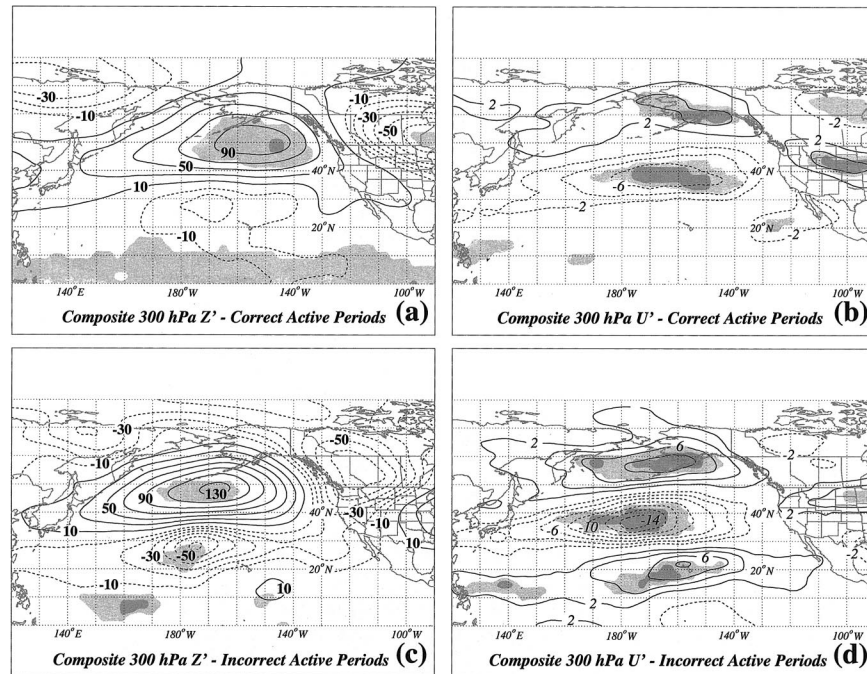


FIG. 9. (a) Composite 300-hPa geopotential height anomalies for correct active periods. Geopotential height is labeled in m with positive (negative) height anomalies contoured as solid (dashed) lines every 20 (10) m beginning at 10 (–10) m. Statistical significance indicated as in Fig. 8a. (b) Composite 300-hPa zonal wind anomalies for correct active periods. Solid (dashed) lines are anomalous isotachs labeled in  $m\ s^{-1}$  with positive (negative) anomalies contoured every 2  $m\ s^{-1}$  starting at 2 (–2)  $m\ s^{-1}$ . Statistical significance indicated as in Fig. 8a. (c) As in (a), but for composite incorrect active periods. (d) As in (b), but for composite incorrect active periods.

posing OLR anomaly dipoles across the tropical Pacific within the composite active and inactive OLR fields.

### b. 300 hPa

The composite 300-hPa height and zonal wind anomalies for correct and incorrect active periods are shown in Fig. 9. Correct active periods are characterized by an anomalous subtropical trough in the central Pacific, an anomalous ridge across the North Pacific, and an anomalous trough over central North America (Fig. 9a). These elements in the height anomaly pattern are reminiscent of the negative phase of the PNA pattern. Since correct active periods are characterized by suppressed tropical convection in the central Pacific (Fig. 8a), the presence of an anomalous subtropical trough and an anomalous midlatitude ridge is consistent with the expected extratropical response due to suppressed tropical convection (Hoskins and Karoly 1981; Ting and Yu 1998). In addition, the orientation of the height anomaly centers along a great circle route is strongly suggestive of Rossby wave dispersion emanating away from the central Pacific, which indicates that anomalous tropical convection near the dateline could be forcing an extratropical response that resembles the PNA pattern. However, with enhanced convection near the date line during

incorrect active periods (Fig. 8b), the same general height anomaly pattern (with a westward shift in the midlatitudes) still develops across the central Pacific and North America with even larger height anomalies in the jet exit region (Fig. 9c) than during correct active periods. This height anomaly pattern is still reminiscent of the negative phase of the PNA pattern, yet is precisely opposite of what might be expected to develop when enhanced tropical convection occurs in the central Pacific. In fact, considering that Rossby wave dispersion theory links enhanced convection in the central Pacific to the development of an anomalous subtropical ridge and an anomalous extratropical trough, the magnitude of these anomalies is even more impressive. The average length of the incorrect active periods (Table 2) precludes the possibility that these height anomalies are a temporary occurrence but rather suggests that in these instances the PNA pattern is simply not forced by tropical convection. Therefore, we conclude that a fully developed PNA-like pattern, associated with an active period of subtropical cyclogenesis, can exist for periods of a week or longer regardless of whether enhanced or suppressed tropical convection occurs in the central Pacific.

As shown in Fig. 9, the development of anomalous height patterns in the central Pacific is also accompanied

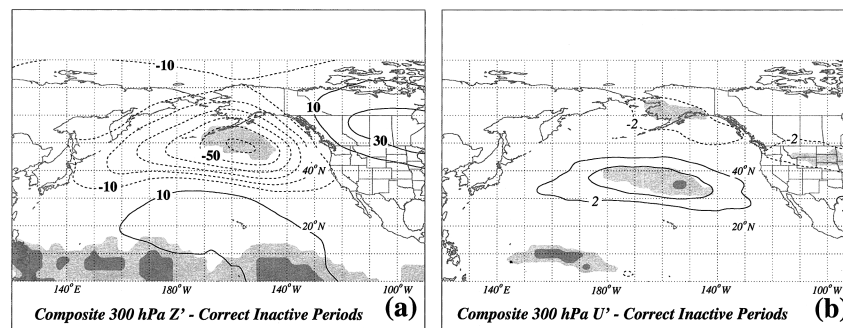


FIG. 10. (a) Composite 300-hPa geopotential height anomalies for correct inactive periods. Geopotential height is labeled in m with positive (negative) height anomalies contoured as solid (dashed) lines every 10 (20) m beginning at 10 (−10) m. Statistical significance indicated as in Fig. 8a. (b) Composite 300-hPa zonal wind anomalies for correct inactive periods. Solid (dashed) lines are anomalous isotachs labeled in  $\text{m s}^{-1}$  with positive (negative) anomalies contoured every 2  $\text{m s}^{-1}$  starting at 2 (−2)  $\text{m s}^{-1}$ . Statistical significance indicated as in Fig. 8a.

by significant<sup>4</sup> changes in the strength and location of the Asian jet. Although both correct (Fig. 9b) and incorrect (Fig. 9d) active periods are characterized by diminished westerlies across the central Pacific, much larger zonal wind anomalies, associated with a significant weakening and westward displacement of the Asian jet, occur during incorrect active periods. The development of highly significant “tripole” pattern in the wind anomaly field during incorrect active periods, characterized by regions of enhanced westerlies over Alaska and the subtropical Pacific and greatly diminished westerlies in the jet exit region, represents a dramatic broadening of the Asian jet across the central Pacific. Given that Hoskins et al. (1983) have indicated that a broadened jet can result from barotropic energy conversions in the exit region of the jet, these observations suggest that barotropic energy conversion may provide a source of energy for cyclone development during these periods.

The composite 300-hPa height and zonal wind anomalies for correct inactive periods are shown in Fig. 10. Correct inactive periods are characterized by an anomalous subtropical ridge in the central Pacific, an anomalous trough in the North Pacific, and an anomalous ridge over central North America (Fig. 10a). Although the anomalies are smaller, this pattern is nearly the polar opposite of the height anomaly pattern that occurs during correct active periods (Fig. 9a) and resembles the positive phase of the PNA pattern. The orientation of the height anomaly centers along a great circle route (similar to those found during correct active periods) suggests that these anomalies could be forced by Rossby wave dispersion away from enhanced tropical convection in the central Pacific (Fig. 8c). This suggestion is supported by the broad resemblance of the present results to those found by Trenberth et al. (1998) during

the 1986/87 El Niño event. It should also be noted that the height anomaly centers in the central Pacific are associated with a zonal extension of the Asian jet (Fig. 10b).

The composite 300-hPa height and zonal wind anomalies associated with incorrect inactive periods are considered next. In the course of construction it became clear that the long-lived incorrect inactive period observed during the winter of 1988/89 (Fig. 2) exerted a disproportionate influence on the resultant composite. Since this period, along with the shorter incorrect inactive period of March 1989, occurred during an extraordinary La Niña event (refer to Fig. 7 of OM), separate composites were constructed for these two “La Niña” periods and for the six “remaining” incorrect inactive periods.

The “La Niña” incorrect inactive periods are characterized by a large region of very strong easterly wind anomalies that extend across much of the SCEP domain (Fig. 11b). This region of highly significant zonal wind anomalies lies between a remarkable height anomaly dipole in the eastern Pacific that consists of an anomalous trough south of Hawaii and an anomalous ridge over the northeastern Pacific (Fig. 11a). Though this dipole is structurally similar to the canonical trough/ridge couplet generally associated with suppressed tropical convection in the central Pacific, the dipole is centered 10 or more degrees farther south than normal. Consequently, the anomalous ridge occupies the northern portion of the SCEP domain, thereby producing an unfavorable environment for cyclone development during these periods.

The composite height and zonal wind anomalies for the six “remaining” incorrect inactive periods are shown in Fig. 12. This composite is characterized by an anomalous extratropical trough that extends across the entire North Pacific basin, an anomalous ridge over western Canada, and a weak anomalous trough over the southeastern United States (Fig. 12a). As was the case

<sup>4</sup> Statistical significance was assessed based upon a one-sided Student's *t* test with a null hypothesis of 0 mean. Further details of the method are given in the appendix.

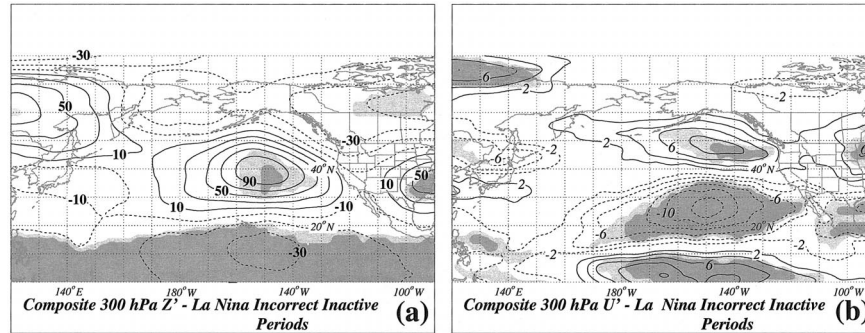


FIG. 11. (a) Composite 300-hPa geopotential height anomalies for the La Niña incorrect inactive periods of 1988/89 (see text for explanation). Geopotential height is labeled and contoured as in Fig. 10a. Statistical significance indicated as in Fig. 8a. (b) Composite zonal wind anomalies for the La Niña incorrect inactive periods of 1988/89. Zonal wind anomalies labeled and contoured as in Fig. 10b. Statistical significance indicated as in Fig. 8a.

for the composite incorrect active periods, this phasing of height anomalies is exactly opposite of what might be expected to develop in the presence of anomalous tropical convection in the central Pacific. This suggests that the presence of suppressed tropical convection in the central Pacific was not a strong influence on the extratropical circulation during these incorrect inactive periods. A plausible explanation for the lack of subtropical cyclones during these periods is provided through an analysis of the zonal wind anomaly field (Fig. 12b), which is dominated by a zonally elongated anomaly dipole that extends across the entire North Pacific basin. The observed dipole is consistent with a narrowing, lengthening, and strengthening of the Asian jet. The corresponding stationary wavenumber field (not shown) indicates that the stronger westerlies are associated with an enhanced waveguide across the Pacific basin. It is therefore suggested that the enhanced waveguide across the Pacific basin associated with the zonally elongated Asian jet acts to limit the propagation and development of upper-level disturbances into the subtropical Pacific, thereby leading to an inactive period.

### c. Adjustment of the 300-hPa height and zonal wind fields during the transition to incorrect active periods

It is interesting to consider the dramatic changes that occur in the upper troposphere during the transition to incorrect active periods. In order to examine this transition, composites were constructed by averaging all of the data during both the 5 days prior to and 5 days after the initiation of each of the eight incorrect active periods. These composites are shown in Fig. 13.

The 5-day prior composites are characterized by a zonally elongated Asian jet (Fig. 13a), a very broad trough across the western two-thirds of the Pacific, and a ridge over western North America (Fig. 13b). After the initiation of an incorrect active period, this entire pattern shifts westward and is characterized by the development of deep troughs over eastern Asia and central North America and a broad ridge across the eastern Pacific (Fig. 13d). The 5-day-after composites are also characterized by the development of a subtropical trough in the central Pacific west of Hawaii (Fig. 13d)

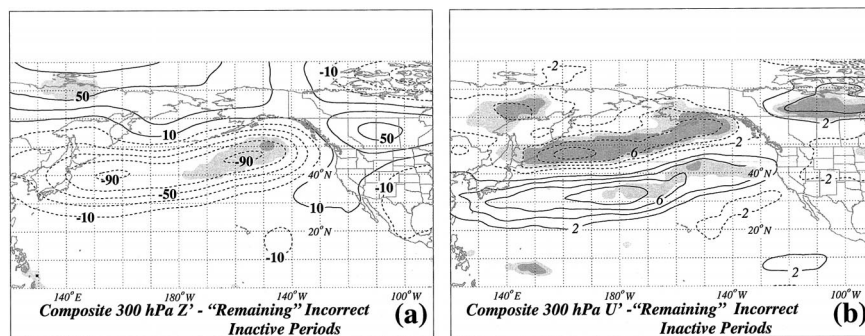


FIG. 12. (a) Composite 300-hPa geopotential height anomalies for the "remaining" incorrect inactive periods (see text for explanation). Geopotential height is labeled and contoured as in Fig. 10a. Statistical significance indicated as in Fig. 8a. (b) Composite zonal wind anomalies for the "remaining" incorrect inactive periods. Zonal wind anomalies labeled and contoured as in Fig. 10b. Statistical significance indicated as in Fig. 8a.

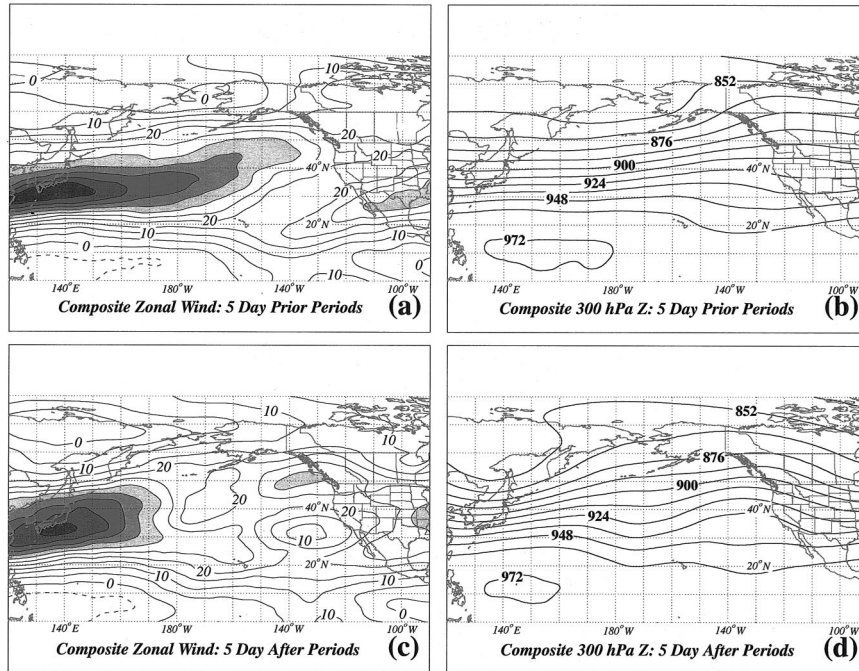


FIG. 13. (a) Composite zonal wind for the 5-day period prior to the start of incorrect active periods. Solid (dashed) lines are isotachs of positive (negative) zonal wind labeled in  $m s^{-1}$  and contoured every  $5 m s^{-1}$ . Shading indicates values greater than  $30 m s^{-1}$ . (b) Composite 300-hPa geopotential height (Z) for the 5-day period prior to the initiation of incorrect active periods. Solid lines are geopotential height lines labeled in dam and contoured every 12 dam. (c) As in (a), but for the 5-day period after the initiation of incorrect active periods. (d) As in (b), but for the 5-day period after the initiation of incorrect active periods.

and by a substantial westward retraction of the Asian jet (Fig. 13c). Therefore, these composites clearly illustrate that a fundamental shift in the large-scale height pattern and a substantial westward retraction of the Asian jet occur after the initiation of the composite incorrect active period.

To better represent these differences, difference fields were calculated by subtracting the 5-day-prior composites from the 5-day-after composites (Fig. 14). Two im-

portant features are evident in Fig. 14. First, the development of substantially weaker westerlies in the jet exit region ( $< -22 m s^{-1}$ ) and stronger westerlies to the north and south after the initiation of an incorrect active period (Fig. 14a) is consistent with the expected response due to barotropic energy conversions in the jet exit region (Hoskins et al. 1983). Second, the height difference field (Fig. 14b) clearly exhibits a PNA-like pattern, which indicates that a rapid transition to the

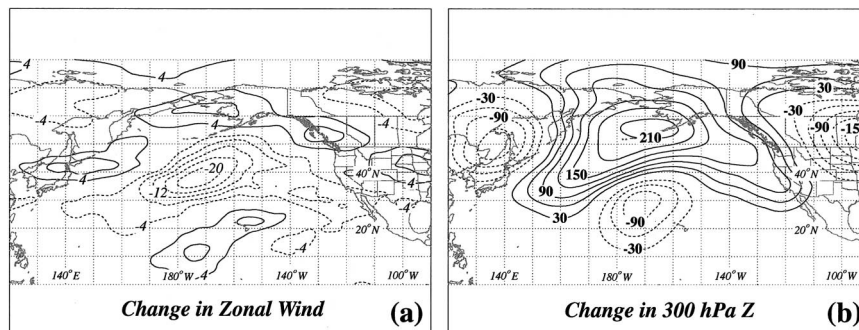


FIG. 14. (a) The 300-hPa zonal wind difference; composite 5-day-after periods minus composite 5-day-prior periods. Solid (dashed) lines indicate isotachs of positive (negative) zonal wind difference labeled in  $m s^{-1}$  and contoured every  $4 m s^{-1}$  starting at  $4 (-4) m s^{-1}$ . (b) The 300-hPa geopotential height difference; composite 5-day-after periods minus composite 5-day-prior periods. Solid (dashed) lines represent positive (negative) geopotential height differences labeled in m and contoured every 30 m beginning at 30 ( $-30$ ) m.

negative phase of the PNA pattern occurs at the beginning of incorrect active periods. Though the careful temporal filtering of data required to comprehensively examine the energetics of such transitions is beyond the scope of the present paper, future work will investigate the local energetics of the composite transition, as well as a representative case study, in order to determine if these energy conversions are associated with barotropic instability in the exit region of the Asian jet.

## 6. Discussion and conclusions

In a recent paper, Otkin and Martin (2004) provided an updated synoptic climatology of subtropical cyclones in the central and eastern Pacific Ocean. Among the results of their climatology was the observation that considerable interannual and intraseasonal variability in subtropical cyclone frequency exists. In the present paper, a detailed investigation of the intraseasonal variability revealed that distinct periods characterized by the frequent or infrequent occurrence of subtropical cyclones (deemed “active” and “inactive” periods, respectively) occur during each cool season. Although the length of these periods varied greatly, they were found to be generally persistent features with an average length of 2 weeks for active periods and 1 month for inactive periods.

In order to examine the large-scale circulation patterns associated with active and inactive periods, composite surface and upper-air analyses were constructed. Examination of these analyses revealed that active periods are characterized by a weak, zonally retracted Asian jet, a weak, westward-shifted Aleutian low, and a broad ridge across the eastern Pacific. Inactive periods, however, are characterized by a strong, zonally elongated Asian jet and a strong Aleutian low. A physical basis for understanding the modulation of subtropical cyclone activity by the Asian jet was provided by an analysis of the stationary wavenumber,  $K_s$ . This analysis demonstrated that the strong, zonally elongated jet characteristic of inactive periods is associated with a continuous waveguide across the Pacific basin that severely limits the equatorward propagation of upper-level cyclones into the subtropical Pacific. Conversely, the zonally retracted jet observed during active periods was associated with a poorly organized, or “leakier,” waveguide across the Pacific, which produces a decidedly more favorable situation for the equatorward propagation of upper-level cyclones leaving the jet exit region. Therefore, this analysis shows that structural changes in the Asian jet can strongly modulate the occurrence of subtropical cyclones in the SCEP by influencing the strength and effectiveness of the midlatitude waveguide across the Pacific.

The identification in the present study of the crucial role played by the Asian jet in modulating the frequency of subtropical cyclone occurrence is consistent with the results of a more limited analysis by Chu et al. (1993).

In an analysis of the large-scale circulation associated with two winters characterized by opposite rainfall anomalies at Honolulu and Lihue, Hawaii, they showed that the wet (dry) season was characterized by a zonally retracted (elongated) Asian jet and by numerous (0) “kona days.” Based upon their limited sample, they also suggested that the PNA pattern may exert a significant control on subtropical cyclone frequency in the Pacific. The presence of a negative PNA pattern during both correct and incorrect active periods and a positive PNA pattern during correct inactive periods robustly confirms the Chu et al. (1993) hypothesis.

A number of empirical studies (e.g., Horel and Wallace 1981; Livezey and Mo 1987; Wang and Fu 2000) have suggested that the PNA pattern is closely linked to the distribution of anomalous tropical convection in the central Pacific. The prevailing conceptual model establishing this link suggests that suppressed (enhanced) tropical convection, presumably associated with the MJO or ENSO, tends to force the negative (positive) phase of the PNA pattern. Theoretical support for this contention resides in the work of Hoskins and Karoly (1981) who used an idealized model to investigate the role of Rossby wave dispersion in forcing an extratropical response far removed from an isolated tropical heat source. In the present study, however, height anomaly fields did not systematically demonstrate the aforementioned relationship between anomalous tropical convection and the phase of the PNA pattern. For instance, 16 active (13 inactive) periods were indeed characterized by the negative (positive) phase of the PNA pattern and suppressed (enhanced) tropical convection in the central Pacific, the expected or “correct” relationship. However, an additional eight active (six inactive; the “remaining” inactive periods illustrated in Fig. 12) periods were broadly characterized by a negative (positive) PNA pattern even though enhanced (suppressed) convection was present in the central Pacific, which represents an “incorrect” relationship. Thus, we conclude that, though forcing by anomalous tropical convection has an important effect on the extratropical circulation during “correct” periods, other processes must account for the presence or absence of subtropical cyclones during “incorrect” periods. This suggests that viewing the PNA pattern primarily as an extratropical response to anomalous tropical forcing in the central Pacific is an oversimplification.

It is suggested that the lack of subtropical cyclones during most of the incorrect inactive periods was a consequence of an enhanced waveguide across the Pacific basin that produced an unfavorable environment for the equatorward propagation of upper-level disturbances into the SCEP. However, for the composite “La Niña” incorrect inactive period, it was the presence of a strong anomalous ridge across the northern portion of the SCEP domain that prohibited cyclone development. The observed broadening and weakening of the Asian jet during the transition to incorrect active periods provides

circumstantial evidence for the role of barotropic energy conversions during such transitions. Future work will document the local energetics of both the composite transition and a case study to provide additional insight into the role of barotropic processes in creating a favorable environment for the development of subtropical cyclones in the SCEP.

Finally, a striking result of the present study is the robust dependence of subtropical cyclone frequency in the North Pacific basin on the strength and zonal extent of the Asian jet. The characteristics of the jet, in turn, appear to derive, in a similarly robust fashion, from the phase of a single regional teleconnection pattern. It is reasonable to imagine whether such simple basic controls on subtropical cyclone frequency operate in the Atlantic Ocean basin or in the Southern Hemisphere subtropical Pacific. Additionally, the evolution of the large-scale circulation associated with periods of enhanced or diminished subtropical cyclone activity in the North Pacific is apparently controlled by several distinct physical mechanisms. Whether or not these mechanisms characteristically work in opposition to, in concert with, or in isolation from one another is a matter for further detailed study.

*Acknowledgments.* The authors thank the European Centre for Medium-Range Weather Forecasts (ECMWF) for generously providing the ECMWF TOGA dataset used in this study. We also thank the NOAA-CIRES Climate Diagnostics Center for supplying the interpolated OLR dataset. The comments of three anonymous reviewers greatly enhanced the presentation of the manuscript. This work was sponsored by the National Science Foundation under Grant ATM-0202012.

## APPENDIX

### Statistical Tests

The statistical tests mentioned in the text were performed using the one-sided Student's  $t$  test:

$$Z = \frac{\bar{x}}{(s^2/N_{\text{eff}})^{1/2}}, \quad (\text{A1})$$

where  $\bar{x}$  is the sample mean,  $s^2$  is the sample variance, and  $N_{\text{eff}}$  is the effective sample size. Here,  $N_{\text{eff}}$  was estimated for each composite grouping using the approximation

$$N_{\text{eff}} \cong \frac{1 - \rho_1}{1 + \rho_1}, \quad (\text{A2})$$

where  $\rho_1$  is the lag 1 autocorrelation evaluated at each grid point in the domain (Wilks 1995, 121–127).

## REFERENCES

- Blackmon, M. I., Y.-H. Lee, and J. M. Wallace, 1984a: Horizontal structure of 500 mb height fluctuations with long, intermediate and short time scales. *J. Atmos. Sci.*, **41**, 961–979.
- , ———, ———, and H.-H. Hsu, 1984b: Time variation of 500 mb height fluctuations with long, intermediate and short time scales as deduced from lag-correlation statistics. *J. Atmos. Sci.*, **41**, 981–991.
- Branstator, G., 1983: Horizontal energy propagation in a barotropic atmosphere with meridional and zonal structure. *J. Atmos. Sci.*, **40**, 1689–1708.
- Businger, S., T. Birchard, K. Kodama, P. Jendrowski, and J.-J. Wang, 1998: A bow echo and severe weather associated with a kona low in Hawaii. *Wea. Forecasting*, **13**, 576–591.
- Cash, B. A., and S. Lee, 2001: Observed nonmodal growth of the Pacific–North American teleconnection pattern. *J. Climate*, **14**, 1017–1028.
- Chu, P.-S., A. J. Nash, and F.-Y. Porter, 1993: Diagnostic studies of two contrasting rainfall episodes in Hawaii: Dry 1981 and wet 1982. *J. Climate*, **6**, 1457–1462.
- Dole, R. M., and R. X. Black, 1990: Life cycles of persistent anomalies. Part II: The development of persistent negative height anomalies over the North Pacific Ocean. *Mon. Wea. Rev.*, **118**, 824–846.
- Feldstein, S. B., 2002: Fundamental mechanisms of the growth and decay of the PNA teleconnection pattern. *Quart. J. Roy. Meteor. Soc.*, **128**, 775–796.
- Geisler, J. E., M. L. Blackmon, G. T. Bates, and S. Munoz, 1985: Sensitivity of January climate response to the magnitude and position of equatorial Pacific sea surface temperature anomalies. *J. Atmos. Sci.*, **42**, 1037–1049.
- Higgins, R. W., and K. C. Mo, 1997: Persistent North Pacific circulation anomalies and the tropical intraseasonal oscillation. *J. Climate*, **10**, 223–244.
- Hoerling, M. P., A. Kumar, and M. Zhong, 1997: El Niño, La Niña, and the nonlinearity of their teleconnections. *J. Climate*, **10**, 1769–1786.
- Horel, J. D., and J. M. Wallace, 1981: Planetary-scale atmospheric phenomena associated with the Southern Oscillation. *Mon. Wea. Rev.*, **109**, 813–829.
- Hoskins, B. J., and D. J. Karoly, 1981: The steady linear response of a spherical atmosphere to thermal and orographic forcing. *J. Atmos. Sci.*, **38**, 1179–1196.
- , and T. Ambrizzi, 1993: Rossby wave propagation on a realistic longitudinally varying flow. *J. Atmos. Sci.*, **50**, 1661–1671.
- , I. N. James, and G. H. White, 1983: The shape, propagation, and mean-flow interaction of large-scale weather systems. *J. Atmos. Sci.*, **40**, 1595–1612.
- Hsu, H.-H., and S.-H. Lin, 1992: Global teleconnections in the 250-mb streamfunction field during the Northern Hemisphere winter. *Mon. Wea. Rev.*, **120**, 1169–1190.
- Kidson, J. W., M. J. Revell, B. Bhaskaran, A. B. Mullan, and J. A. Renwick, 2002: Convection patterns in the tropical Pacific and their influence on the atmospheric circulation at higher latitudes. *J. Climate*, **15**, 137–159.
- Kiladis, G. N., 1998: Observations of Rossby waves linked to convection over the eastern tropical Pacific. *J. Atmos. Sci.*, **55**, 321–339.
- , and K. M. Weickmann, 1997: Horizontal structure and seasonality of large-scale circulations associated with submonthly tropical convection. *Mon. Wea. Rev.*, **125**, 1997–2013.
- Knutson, T. R., and K. M. Weickmann, 1987: 30–60 day atmospheric oscillations: Composite life cycles of convection and circulation anomalies. *Mon. Wea. Rev.*, **115**, 1407–1436.
- Kodama, K., and G. M. Barnes, 1997: Heavy rain events over the south-facing slopes of Hawaii: Attendant conditions. *Wea. Forecasting*, **12**, 347–367.
- Kousky, V. E., 1985: Seasonal climate summary: The global climate for December 1984–February 1985: A case of strong intraseasonal oscillations. *Mon. Wea. Rev.*, **113**, 2158–2172.
- Lau, K.-M., and T. J. Phillips, 1986: Coherent fluctuations of extratropical geopotential height and tropical convection in intraseasonal time scales. *J. Atmos. Sci.*, **43**, 1164–1181.
- Liebmann, B., and C. A. Smith, 1996: Description of a complete

- (interpolated) outgoing longwave radiation dataset. *Bull. Amer. Meteor. Soc.*, **77**, 1275–1277.
- Livezey, R. E., and K. C. Mo, 1987: Tropical–extratropical teleconnections during the Northern Hemisphere winter. Part II: Relationships between monthly mean Northern Hemisphere circulation patterns and proxies for tropical convection. *Mon. Wea. Rev.*, **115**, 3115–3132.
- Lyons, S. W., 1982: Empirical orthogonal function analysis of Hawaiian rainfall. *J. Appl. Meteor.*, **21**, 1713–1729.
- Martin, J. E., and J. A. Otkin, 2004: The rapid growth and decay of an extratropical cyclone in the central Pacific Ocean. *Wea. Forecasting*, **19**, 358–376.
- Matthews, A. J., and G. N. Kiladis, 1999: The tropical–extratropical interaction between high-frequency transients and the Madden–Julian Oscillation. *Mon. Wea. Rev.*, **127**, 661–677.
- Morrison, I., and S. Businger, 2001: Synoptic structure and evolution of a kona low. *Wea. Forecasting*, **16**, 81–98.
- Otkin, J. A., and J. E. Martin, 2004: A synoptic climatology of the subtropical kona storm. *Mon. Wea. Rev.*, **132**, 1502–1517.
- Ramage, C. S., 1962: The subtropical cyclone. *J. Geophys. Res.*, **67**, 1401–1411.
- Schubert, S. S., and C.-K. Park, 1991: Low-frequency intraseasonal tropical–extratropical interactions. *J. Atmos. Sci.*, **48**, 629–650.
- Simmons, A. J., J. M. Wallace, and G. W. Branstator, 1983: Barotropic wave propagation and instability, and atmospheric teleconnection patterns. *J. Atmos. Sci.*, **40**, 1363–1392.
- Simpson, R. H., 1952: Evolution of the kona storm, a subtropical cyclone. *J. Meteor.*, **9**, 24–35.
- Ting, M., and L. Yu, 1998: Steady response to tropical heating in wavy linear and nonlinear baroclinic models. *J. Atmos. Sci.*, **55**, 3565–3582.
- Trenberth, K. E., G. W. Branstator, D. Karoly, A. Kumar, N.-C. Lau, and C. Ropelewski, 1998: Progress during TOGA in understanding and modeling global teleconnections associated with tropical sea surface temperatures. *J. Geophys. Res.*, **103**, 14 291–14 324.
- Wallace, J. M., and D. M. Gutzler, 1981: Teleconnections in the geopotential height field during the Northern Hemisphere winter. *Mon. Wea. Rev.*, **109**, 784–812.
- Wang, H., and R. Fu, 2000: Winter monthly mean atmospheric anomalies over the North Pacific and North America associated with El Niño SSTs. *J. Climate*, **13**, 3435–3447.
- Wang, J.-J., H.-M. Juang, K. Kodama, S. Businger, Y.-L. Chen, and J. Partain, 1998: Application of the NCEP Regional Spectral Model to improve mesoscale weather forecasts in Hawaii. *Wea. Forecasting*, **13**, 560–575.
- Weickmann, K. M., G. R. Lussky, and J. E. Kutzbach, 1985: Intra-seasonal (30–60 day) fluctuations of outgoing longwave radiation and 250 mb streamfunction during northern winter. *Mon. Wea. Rev.*, **113**, 941–961.
- Wilks, D. S., 1995: *Statistical Methods in the Atmospheric Sciences*. Academic Press, 467 pp.
- Yang, G.-Y., and B. J. Hoskins, 1996: Propagation of Rossby waves of nonzero frequency. *J. Atmos. Sci.*, **53**, 2365–2378.